The transformation between τ and TCB for deep space missions under IAU resolutions[*]

Xue-Mei Deng

Purple Mountain Observatory, Chinese Academy of Sciences, Nanjing 210008, China;
xmd@pmo.ac.cn

Abstract For tracking spacecraft and performing radio science, the transformation between the proper time (τ) given by a clock carried onboard a spacecraft and the barycentric coordinate time (TCB) is investigated under IAU resolutions. In order to more clearly demonstrate manifestations of a physical model and improve computational efficiency, an analytic approach is adopted. After numerical verification, it is confirmed that this method is adequate to describe a Mars orbiter during one year, and is particularly good at describing the influence from perturbing bodies. Further analyses demonstrate that there are two main effects in the transformation: the gravitational field of the Sun and the velocity of the spacecraft in the barycentric coordinate reference system. The combined contribution of these effects is at the level of a few sub-seconds.

Key words: reference systems — time — method: analytical — method: numerical — space vehicles

1 INTRODUCTION

The last few decades have seen enormous improvements in the accuracy of measurements and unprecedented progress in measurement techniques. This makes the the effects of general relativity (GR) become an indispensable part of data processing in high-precision observations. Thus, the first order post-Newtonian (1PN) general relativistic theory of astronomical reference frames, based on Brumberg & Kopejkin (1989) and Damour et al. (1991), was adopted by the General Assembly of the International Astronomical Union (IAU) in 2000 (Soffel et al. 2003). Likewise, GR plays an important role in deep space missions in terms of navigation and scientific experiments.

For example, the radio link connecting a spacecraft and a ground station has been a sensitive and useful tool for probing the interior structure of a body in the solar system. Some signals from these intriguing but subtle effects might become entangled with those due to curved spacetime. This work is therefore the first step towards constructing an applicable and consistent relativistic framework that will be able to separate planetary information from GR "bias." On the other hand, the radio link in interplanetary space missions could test theories of gravity. In 2003, the Cassini spacecraft had confirmed GR to an accuracy of 10^{-5} by Doppler tracking in the spacecraft's solar conjunction

(Bertotti et al. 2003). This result not only verified GR, but also ruled out some of the theories which did not satisfy the corresponding conditions. Deep space missions might also open a new window on some new physical laws at the scale of the solar system, uncovering the challenge of unexplained anomalies (Anderson et al. 1998, 2008). This is the reason why a complete data reduction framework should be established robustly in the first place to interpret the associated observational data.

A general scheme for data reduction based on a relativistic framework is presented as follows. Starting from a Lagrangian based theory of gravity, the metric of the solar system can be obtained by a post-Newtonian approximation (Chandrasekhar 1965). A global reference system covering the whole spacetime region is introduced to describe the orbital motions of bodies in the solar system. Some local reference systems are also introduced and each of them covers a region near a body to define the multiple moments of the body and describe the motions of its massless satellites. However, most of the current data reduction methods, including lunar laser ranging, are conducted in the global frame. Thus, this involves a coordinate transformation between the global frame and a local one. This transformation has been intensively studied by Brumberg & Kopejkin (1989), Damour et al. (1991), Klioner & Soffel (2000), Kopeikin & Vlasov (2004) and Xie & Kopeikin (2010). Within this relativistic framework, the motions of spacecraft, celestial bodies, light rays (photons) and observers in the solar system would be adequately represented in different reference frames. The task is to make a relativistic model for a specific kind of observation with some physical or conventional quantities.

In the above process, different time scales exist within the relativistic framework, in contrast to Newton's idea of absolute spacetime. A clock onboard a spacecraft gives the proper time τ, which is a physical time. To deal with the propagation of the signals emitted by a spacecraft in the solar system, the Barycentric Celestial Reference System (BCRS) is usually used. This has a coordinate time component, called the barycentric coordinate time (TCB). Therefore τ needs to be connected to TCB during the whole radio link. This is one of the motivations for our research work. In general, a numerical method or an analytic one could be adopted to discuss this transformation. Although the numerical method is more feasible for computation, inversion and prediction of astronomical events and phenomena, it is not enough to provide some of the physical information. With a practical case in hand, the method cannot distinguish the leading terms, the secular terms accumulated with time and the negligible terms from the numerical results. Besides, the presence of hundreds of terms using higher order approximation (for example, from 1PN to 2PN) makes these problems more complicated. However, the analytic method is extraordinarily good at these. In particular, the computational process of the analytic method saves time and is more efficient. From the gauge-invariant point of view, some spurious coordinate-dependent effects can be removed by the analytic method. Thus a more efficient and unambiguous method can be found that provides the above advantages, and this is the other motivation for this paper.

As a first step, by employing an analytic method, this work mainly focuses on the transformation between the proper time τ on the spacecraft and TCB under IAU resolutions. It shows that there is a difference in the two time systems between the one on the spacecraft and the global system. This transformation will be applied to connect the emitted signal with the light propagation and can also be applied to tracking, telemetry and control at the ground stations.

We will summarize some of the conventions and notations used in this paper. The metric signature is $(-, +, +, +)$; G is the Newtonian constant of gravitation; c is the velocity of light and $\epsilon \equiv 1/c$; the capital subscripts A, B, $C \ldots$ refer to the gravitating bodies in the solar system; the subscripts T and s denote, respectively, the quantities related to the target body and the spacecraft; the Latin indices $i, j, k \ldots$ denote three-dimensional space components; the symmetric and trace-free (STF) part of the tensor I^{ij} is denoted by $I^{<ij>}$; we also use multi-index notations such as $I^{<L>} \equiv I^{<i_1 i_2 \ldots i_l>}$. Section 2 is devoted to an analytic expression for the transformation between τ and TCB under IAU resolutions. Considering a Mars mission, a comparison between the numerical method and our analytic one is described in Section 3. Then, in Section 4, some results are derived with our analytic method. Finally, the conclusion and discussion are outlined in Section 5.

2 MODEL AND ANALYTIC EXPRESSION

In BCRS, the metric tensor under IAU resolutions (Soffel et al. 2003) reads as

$$g_{00} = -1 + \epsilon^2 2w - \epsilon^4 2w^2 + \mathcal{O}(5), \tag{1}$$
$$g_{0i} = -\epsilon^3 4w^i + \mathcal{O}(5), \tag{2}$$
$$g_{ij} = \delta_{ij}(1 + \epsilon^2 2w) + \mathcal{O}(4), \tag{3}$$

where w and w^i are, respectively, scalar and vector potentials, and $\mathcal{O}(n)$ means of the order ϵ^n. Then, the transformation between the proper time of a spacecraft τ_s and TCB(t) can be done by integrating the following equations

$$\frac{\mathrm{d}\tau_\mathrm{s}}{\mathrm{d}t} = 1 - \epsilon^2\left(w + \frac{1}{2}v_\mathrm{s}^2\right) + \epsilon^4\left(\frac{1}{2}w^2 + 4w^k v_\mathrm{s}^k - \frac{3}{2}wv_\mathrm{s}^2 - \frac{1}{8}v_\mathrm{s}^4\right) + \mathcal{O}(5). \tag{4}$$

In principle, w and w^i should be expressed as the local multipole moments. However, if we only consider N-point masses with spins, Equation (4) yields

$$\begin{aligned}
\frac{\mathrm{d}\tau_\mathrm{s}}{\mathrm{d}t} = 1 - \epsilon^2&\left(\sum_A \frac{Gm_A}{r_{\mathrm{s}A}} + \frac{1}{2}v_\mathrm{s}^2\right) \\
-\epsilon^4&\left[\frac{1}{8}v_\mathrm{s}^4 - \frac{1}{2}\sum_A \frac{G^2 m_A^2}{r_{\mathrm{s}A}^2} + 2\sum_A \frac{Gm_A}{r_{\mathrm{s}A}}v_A^2 + \frac{3}{2}\sum_A \frac{Gm_A}{r_{\mathrm{s}A}}v_\mathrm{s}^2\right. \\
&- \frac{1}{2}\sum_A \frac{Gm_A}{r_{\mathrm{s}A}^3}(r_{\mathrm{s}A}^k v_A^k)^2 - 4\sum_A \frac{Gm_A}{r_{\mathrm{s}A}}v_\mathrm{s}^k v_A^k \\
&- 4\sum_A \frac{G}{r_{\mathrm{s}A}^3}\varepsilon_{ij}^k S_A^i r_{\mathrm{s}A}^j v_\mathrm{s}^k - \frac{1}{2}\sum_A \sum_{B \neq A} \frac{G^2 m_A m_B}{r_{\mathrm{s}A}r_{\mathrm{s}B}} \\
&\left.- \sum_A \sum_{B \neq A} \frac{G^2 m_A m_B}{r_{\mathrm{s}A}r_{AB}} + \frac{1}{2}\sum_A \sum_{B \neq A} \frac{G^2 m_A m_B}{r_{\mathrm{s}A}r_{AB}^3}r_{\mathrm{s}A}^k r_{AB}^k\right],
\end{aligned} \tag{5}$$

where 1PN masses are obtained by using the method of two effective time-dependent masses of the A-th body

$$\tilde{\mu}_A = m_A\left\{1 + \epsilon^2\left[-\sum_{B \neq A}\frac{Gm_B}{r_{AB}} + \frac{3}{2}v_A^2\right]\right\} + \mathcal{O}(4), \tag{6}$$

$$\mu_A = m_A\left\{1 + \epsilon^2\left[-\sum_{B \neq A}\frac{Gm_B}{r_{AB}} + \frac{1}{2}v_A^2\right]\right\} + \mathcal{O}(4), \tag{7}$$

based on Blanchet et al. (1998). Here $r_{\mathrm{s}A} = |\boldsymbol{x}_\mathrm{s} - \boldsymbol{x}_A|$ and $r_{AB} = |\boldsymbol{x}_A - \boldsymbol{x}_B|$; $\boldsymbol{x}_\mathrm{s}$ and $\boldsymbol{x}_A$, respectively, denote the positions of the spacecraft and the A-th body in BCRS. $\boldsymbol{v}_\mathrm{s}$ and $\boldsymbol{v}_A$, respectively, denote the velocities of the spacecraft and the A-th body in BCRS. ε_{ij}^k is the fully antisymmetric Levi-Civita symbol and S_A^i is the spin of the A-th body. In this paper, we mainly consider the effects of the terms in Equation (5) on the order of ϵ^2 on the transformation. Namely,

$$\frac{\mathrm{d}\tau_\mathrm{s}}{\mathrm{d}t} = 1 - \epsilon^2\left(\sum_A \frac{Gm_A}{r_{\mathrm{s}A}} + \frac{1}{2}v_\mathrm{s}^2\right) + \mathcal{O}(\epsilon^4). \tag{8}$$

The first term on the order of ϵ^2 is a dynamical term which is contributed from the N-body's gravitational fields. The second term in Equation (8) on the order of ϵ^2 is a kinematic term which comes from the velocity of the spacecraft. For the dynamical term, we split it into two parts

$$\sum_A \frac{Gm_A}{r_{\mathrm{s}A}} = \sum_{A \neq T} \frac{Gm_A}{r_{\mathrm{s}A}} + \frac{Gm_T}{r_{\mathrm{s}T}}, \tag{9}$$

where the first one comes from the contribution of perturbing bodies and the second is caused by the target body of the deep space mission. There exists a small quantity $q \equiv r_{\mathrm{s}T}/r_{AT}$, which describes the distance between the spacecraft and the target body divided by the distance between the target body and the perturbing body. For the perturbing terms, they can be expanded by q^k ($k = 0, 1, 2, \ldots$) and become

$$\begin{aligned}
\sum_{A \neq T} \frac{Gm_A}{r_{\mathrm{s}A}} &= \sum_{A \neq T} \frac{Gm_A}{|\boldsymbol{x}_A - \boldsymbol{x}_T - (\boldsymbol{x}_{\mathrm{s}} - \boldsymbol{x}_T)|} \\
&= \sum_{A \neq T} \sum_{k=0}^{l} \frac{(2k-1)!!}{k!} \frac{Gm_A}{r_{AT}^{2k+1}} r_{AT}^{<K>} r_{\mathrm{s}T}^{<K>} + \mathcal{O}(\sum_{k=l+1}^{\infty}) \\
&= \underbrace{\sum_{A \neq T} \frac{Gm_A}{r_{AT}}}_{l=0} + \underbrace{\sum_{A \neq T} \frac{Gm_A}{r_{AT}^3} r_{AT}^k r_{\mathrm{s}T}^k + \frac{3}{2} \sum_{A \neq T} \frac{Gm_A}{r_{AT}^5} r_{AT}^{<i} r_{AT}^{j>} r_{\mathrm{s}T}^{<i} r_{\mathrm{s}T}^{j>} + \mathcal{O}(\sum_{k=3}^{\infty})}_{l=2}. \tag{10}
\end{aligned}$$

For the dynamical term representing perturbations, the above analytic expression will converge with an the increase in the index k. In our research, we mainly focus on the first three terms, which correspond to $l = 2$. In the next section, we will prove that the difference between the analytic method and the numerical one for the perturbations is negligible with respect to the current accuracy of measurements.

Our task is to derive the analytic expression of Equation (8) to the order of ϵ^2. The positions and velocities of the bodies and the spacecraft in the solar system are obtained by treating them as N two-body problems. For example, the motions of eight planets with respect to the Sun are considered as eight two-body problems, and the motion of the spacecraft with respect to its target body is also considered as a two-body problem. For planet A, its position $\boldsymbol{r}_A^{\mathrm{Heli}}$ and velocity $\boldsymbol{v}_A^{\mathrm{Heli}}$ are expressed with the orbital elements in the heliocentric coordinate system as a two-body problem (Murray & Dermott 2000). These elements change with time, such as $a_A = a_{A0} + \dot{a}_A T_{\mathrm{eph}}$, $e_A = e_{A0} + \dot{e}_A T_{\mathrm{eph}}$ and so on, based on table 1 in the technical report of JPL (Standish et al. 1992), where T_{eph} is the number of centuries past J2000.0. With the positions and velocities of eight planets in the heliocentric coordinate system obtained, the position and velocities of the solar system's barycenter (SSB) in the heliocentric coordinate system are then, respectively, obtained by $\sum_A m_A \boldsymbol{r}_A^{\mathrm{Heli}}/\sum_A m_A$ and $\sum_A m_A \boldsymbol{v}_A^{\mathrm{Heli}}/\sum_A m_A$. Using the positions of the planets and SSB in the heliocentric coordinate system, we can obtain the positions and the velocities of the Sun, Mercury, Venus, the Earth-Moon Barycenter (EMB), Mars, Jupiter, Saturn, Uranus and Neptune in BCRS. For $r_{\mathrm{s}T}^i$, we can solve this from the two-body problem in the equatorial reference system of the target body (Murray & Dermott 2000). Furthermore, we rotate vector $r_{\mathrm{s}T}^i$ from the equatorial reference system to the International Celestial Reference System (ICRS) based on the procedures recommended by the IAU/IAG Working Group on cartographic coordinates and rotational elements (Archinal et al. 2011). The above proposed rotations are derived to deal with the coupling terms with vectors calculated in different reference systems.

Table 1 Components in $\tau_s - t$

	Max (s)	Order		Max (s)	Order		Max (s)	Order
Sun	0.2	c^{-2}	Mercury	4×10^{-8}	c^{-2}	EMB	4×10^{-7}	c^{-2}
Sun	7×10^{-10}	c^{-4}	Venus	6×10^{-7}	c^{-2}	Mars	3×10^{-4}	c^{-2}
Jupiter	7×10^{-5}	c^{-2}	Uranus	7×10^{-7}	c^{-2}	$\int \frac{1}{2} v_s^2 dt$	0.1	c^{-2}
Saturn	8×10^{-6}	c^{-2}	Neptune	5×10^{-7}	c^{-2}	$\int \frac{1}{8} v_s^4 dt$	2×10^{-10}	c^{-4}

For the kinematic term of Equation (8), we only focus on the two-body interactions and omit perturbations of the other bodies

$$
\begin{aligned}
v_s^2 &= (\boldsymbol{V}_s + \boldsymbol{v}_T) \cdot (\boldsymbol{V}_s + \boldsymbol{v}_T) + \mathcal{O}(\epsilon^2, \text{others}) \\
&= v_T^2 + V_s^2 + 2\boldsymbol{v}_T \cdot \boldsymbol{V}_s + \mathcal{O}(\epsilon^2, \text{others}) \\
&= Gm_\odot \left(\frac{2}{r_{T\odot}} - \frac{1}{a_T} \right) + Gm_T \left(\frac{2}{r_{sT}} - \frac{1}{a_s} \right) + 2\boldsymbol{v}_T \cdot \boldsymbol{V}_s + \dots,
\end{aligned}
\tag{11}
$$

where subscripts "s," "$\odot$" and "T" denote the terms related to the spacecraft, the Sun and the target body, respectively, $\boldsymbol{v}_T$ denotes the velocity vector of the target body in BCRS, and $\boldsymbol{V}_s$ denotes the velocity vector of the spacecraft in the target body's local reference system. For $\boldsymbol{v}_T \cdot \boldsymbol{V}_s$ in Equation (11), we must put the two vectors in the same coordinate system as BCRS. $\boldsymbol{V}_s$ can be written as $(V_s, 0, 0)^T$ in the (U, N, W) triad, where U points to the direction tangent to the orbit. Furthermore, we rotate this vector to the (S, T, W) triad, where S points to the radial direction, then to the equatorial plane of the target body and finally to BCRS. Such a transformation is performed by $R_3(-90° - \alpha_T)R_1(\delta_T - 90°)R_3(-\Omega)R_1(-i)R_3(-\omega - f)R_3(\theta)(V_s, 0, 0)^T$, where α_T and δ_T are ICRF equatorial coordinates at epoch J2000.0 for the north pole of one target body; Ω denotes the longitude of the ascending node for the spacecraft; i denotes the inclination of the orbit for the spacecraft; ω denotes the longitude of the periastron for the spacecraft; f is the true anomaly; θ is the angle between the tangent direction and transverse direction of the orbit, and $\cos\theta = (1 + e\cos f)/\sqrt{1 + 2e\cos f + e^2}$.

Then, the analytic relation between τ_s and t is

$$
\begin{aligned}
\tau_s - t = -\epsilon^2 & \int \left[\sum_{A \neq T} \frac{Gm_A}{r_{AT}} + \sum_{A \neq T} \frac{Gm_A}{r_{AT}^3} r_{AT}^k r_{sT}^k + \frac{3}{2} \sum_{A \neq T} \frac{Gm_A}{r_{AT}^5} r_{AT}^{<i} r_{AT}^{j>} r_{sT}^{<i} r_{sT}^{j>} + \frac{Gm_T}{r_{sT}} \right] dt \\
& -\epsilon^2 \int \left[Gm_\odot \left(\frac{1}{r_{T\odot}} - \frac{1}{2a_T} \right) + Gm_T \left(\frac{1}{r_{sT}} - \frac{1}{2a_s} \right) + \boldsymbol{v}_T \cdot \boldsymbol{V}_s \right] dt \\
& + \mathcal{O}(\epsilon^2, l \geq 3, \text{others}),
\end{aligned}
\tag{12}
$$

where the positions and velocities of the N-body and the spacecraft can be easily obtained by the solutions of the two-body problem. Compared to the numerical method, this analytic approach is more efficient in terms of computation. In the next section, we will prove that this approach is satisfactory by performing the numerical check.

3 NUMERICAL CHECK

In this section, we will check our analytic result by comparison with the numerical results under the requirements for a Mars mission. We simulate a spacecraft that has a very large elliptical orbit around Mars from 2012 Nov. 01 to 2013 Nov. 01. Its orbital inclination to the Martian equator is about 5°. The apoapsis altitude is $80\,000$ km and the periapsis altitude is 800 km, with a period of about 3 days.
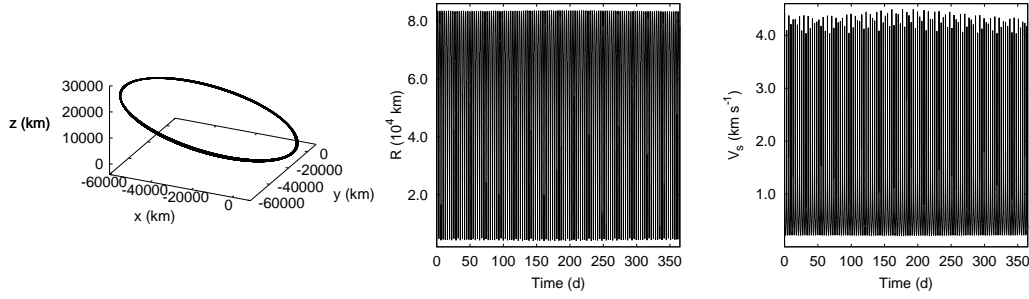
Fig. 1 *Left*: 3D orbital motion of the spacecraft probing Mars (in km). *Middle*: the distance R (in km) between the center of Mars and the spacecraft versus time (in day). *Right*: the velocity of the spacecraft V_{s} (in km s^{-1}) with respect to the center of mass of Mars versus time (in day).

In the simulation, the positions and velocities of the planets and the Sun are read from the ephemeris DE405. The initial conditions of the spacecraft are calculated from its orbital elements in the Martian equatorial reference frame, and transferred into ICRS for numerical integration. For a one year mission, the precession and nutation are negligible in the rotational elements of Mars for this transformation, so we only consider the fixed term for the north pole of Mars, namely, $\alpha_0 = 317.68143°$ and $\delta_0 = 52.88650°$ (see Archinal et al. 2011). The integrator we use is RKF7(8) (Fehlberg 1968) with a fixed step-size of 30 minutes.

In Figure 1, our numerical results for the spacecraft are displayed. The left panel shows its 3D orbit and we can see a large ellipse. The middle shows the change in its distance from Mars with time, where we can see the maximum and the minimum values of R. The right panel shows its velocity with respect to the center of mass of Mars. With the position $\boldsymbol{x}_{\mathrm{s}}$ and velocity $\boldsymbol{v}_{\mathrm{s}}$ of the spacecraft in BCRS, we can numerically calculate

$$\tau_{\mathrm{s}} - t = -\epsilon^2 \int \left(\sum_A \frac{Gm_A}{r_{\mathrm{s}A}} + \frac{1}{2} v_{\mathrm{s}}^2 \right) \mathrm{d}t. \tag{13}$$

Since being obtained from DE405, the positions of the planets depend on the coordinate time of the planetary ephemeris: Barycentric Dynamical Time (TDB). The relationship between TDB and TCB is TDB $= (1 - L_B)$TCB with $L_B = 1.550519768 \times 10^{-8}$ according to IAU resolutions (Petit & Luzum 2010). However, this influence of L_B could be negligible because it is coupled with ϵ^2.

With these numerical results, we can check our analytic approach. Firstly, we consider the effects of the dynamical term. For perturbations, there are three terms in the analytic expression (see Eq. (12)). We introduce a dimensionless quantity δ_A for contribution A in $\tau_{\mathrm{s}} - t$, which is defined as $\delta_A \equiv [\text{analytic (A)} - \text{numerical (A)}]/[\text{numerical } (\tau_{\mathrm{s}} - t)]$.

Figure 2 shows δ_A of the Sun, Mercury, Venus, EMB, Jupiter, Saturn, Uranus and Neptune for $l = 0$, $l = 1$ and $l = 2$. The contributions of perturbations are well described by our analytic approach because δ_A decreases to $\sim 10^{-12}$ or below with $l = 2$. Although the curves of Figure 2 have some fluctuation at the beginning, they tend to smooth with time. For the effect of Mars in the dynamical term, the left panel of Figure 3 displays a comparison between the numerical and the analytic results. The maximum δ_{Mars} is about 10^{-7}. The right panel of Figure 3 shows a numerical check of the kinematic term and $\delta_{v_{\mathrm{s}}^2}$ is about 10^{-5}. Both of these are caused by the fact that pure two-body problem solutions are adopted in our analytic approach, but full N-body integration is used in the numerical simulation.
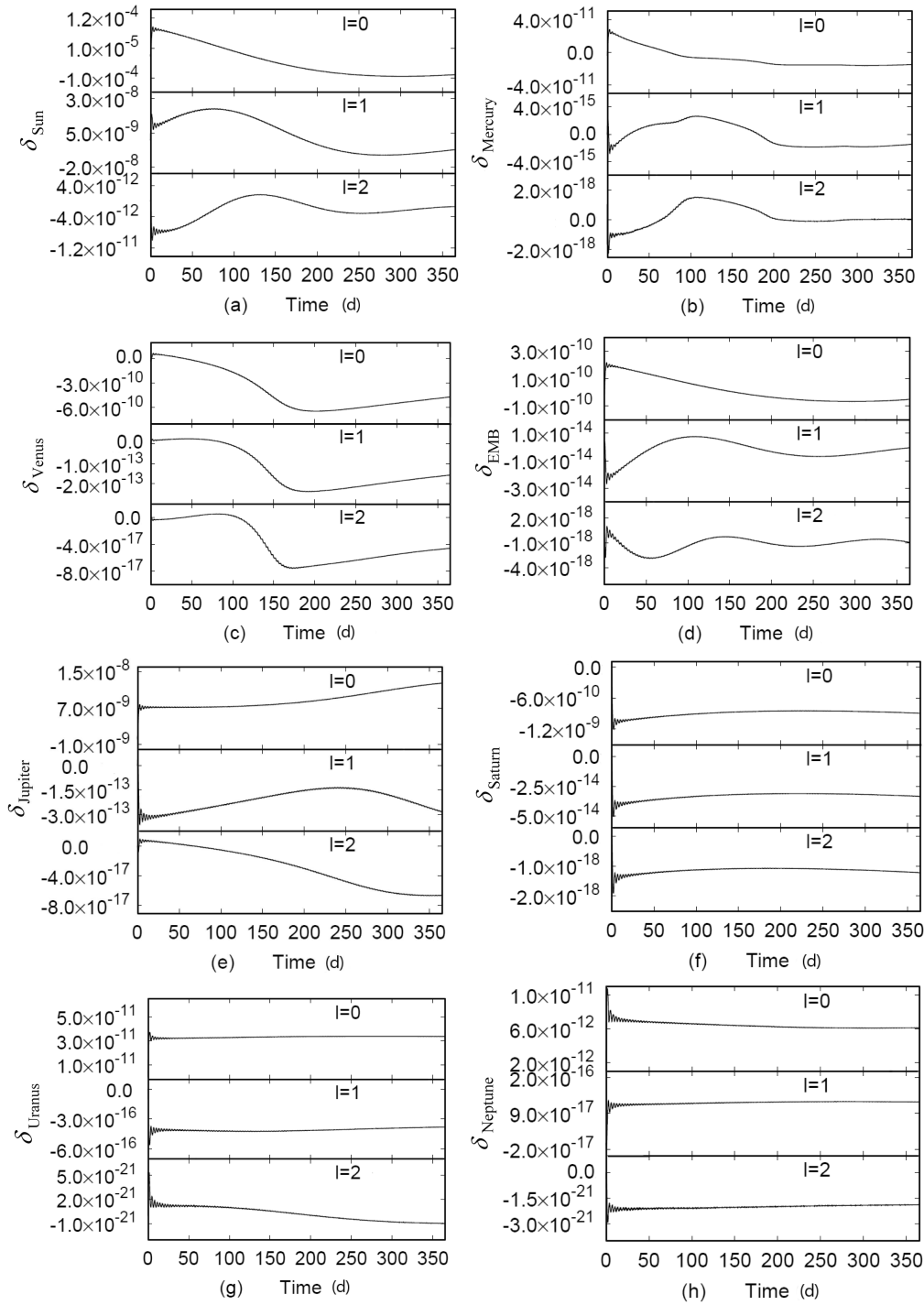
Fig. 2 Normalized relative deviation between the analytic and numerical results δ_A for perturbing bodies with $l = 0$, 1 and 2 versus the integrated time (in day). (a) for the Sun; (b) Mercury; (c) Venus; (d) the EMB; (e) Jupiter; (f) Saturn; (g) Uranus; and (h) Neptune.
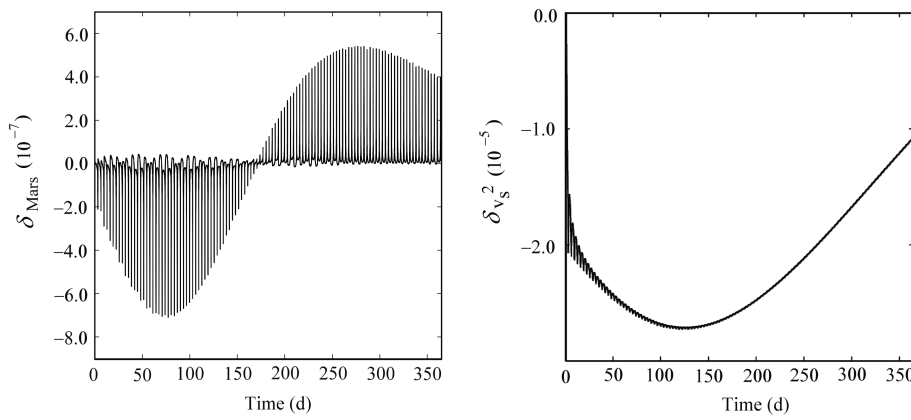
Fig. 3 *Left*: the normalized relative deviation for Mars versus the integrated time (in day). *Right*: the normalized relative deviation for the velocity of the spacecraft in the BCRS versus the integrated time (in day).
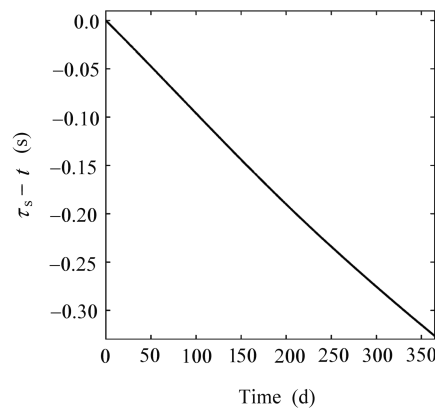
Fig. 4 Difference in $\tau_s - t$ with time.

4 ANALYTIC RESULTS

Some of the results are derived with our analytic method after verification by the numerical check. Figure 4 shows the curve of $\tau_s - t$ computed by Equation (12). We can see that the difference between the proper time and TCB could reach the level of sub-seconds. This effect has two main components: the Sun's gravitational field and the velocity of the spacecraft in the BCRS.

Figure 5(a)–(j) displays the contributions of the Sun, Mercury, Venus, the EMB, Mars, Jupiter, Saturn, Uranus, Neptune and the velocity of the spacecraft (i.e. $-\epsilon^2 \int v_s^2/2\mathrm{d}t$). Since the Sun's gravitational field and the velocity of the spacecraft in BCRS dominate, we further consider these contributions in the next order, namely, $\epsilon^4 \int G^2 m_\odot^2/(2r_{s\odot}^2)\mathrm{d}t$ and $-\epsilon^4 \int v_s^4/8\mathrm{d}t$ (see Fig. 5(k) and Fig. 5(l)). These two terms on the order of ϵ^4 are very small, around $\sim 10^{-10}$s.

Table 1 gives the maximum values of different effects in the term $\tau_s - t$. On the order of ϵ^2, the Sun's gravitational field and the velocity of the spacecraft have contributions up to a few sub-seconds, while the others belong to the microsecond-level or below. On the order of ϵ^4, the maximum contributions of the Sun's gravitational field and the velocity of the spacecraft are at the level of 0.1 nanoseconds. This means that if we take 1 nanosecond as the precision of the time system, the
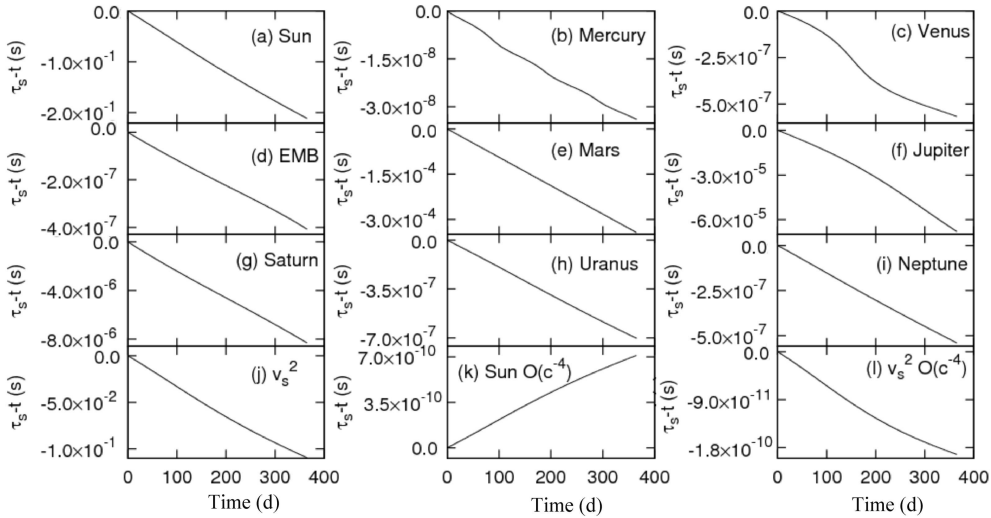
Fig. 5 Different terms in Eq. (12) versus time. Panels (a)–(j) denote the contributions from the Sun, Mercury, Venus, the EMB, Mars, Jupiter, Saturn, Uranus, Neptune and v_s^2 on the order of c^{-2}, respectively. Panels (k) and (l) respectively denote the effects of the Sun and the velocity of the spacecraft in terms of $\tau_s - t$ on the order of c^{-4}.

transformation between the proper time on the spacecraft and TCB only needs to include the terms on the order of ϵ^2.

If we take the YingHuo-1 Mission as a technical example of future Chinese Mars explorations, the proposed spacecraft would be equipped with a clock such as the ultra-stable-oscillator (USO), whose instability is less than values in the range 1×10^{-12} to 2×10^{-12} for time spans from 0.1 to 1000 s (Ping et al. 2009). Accuracy control must be performed for the clock carried onboard because its accuracy will drift for various reasons. Thus, it is almost impossible to estimate the timing error of a clock after one year in terms of its stability or accuracy, and we only discuss a time span within a one year mission, such as one month. $\tau_s - t$ can maintain a level of accuracy of 10^{-2} s within one month of operation. At the level of a microsecond (10^{-6} s) of timing accuracy, although δ_{Mars} and $\delta_{v_s^2}$ could maximally reach 10^{-7} and 10^{-5}, their maximum contributions to the deviation of $\tau_s - t$ are, respectively, 10^{-9} s and 10^{-7} s for one month of operation, and both of them are less than 10^{-6} s. This shows that our analytical approach is satisfactory for a Mars orbiter.

5 CONCLUSIONS

In this paper, the transformation between the proper time on a spacecraft and the TCB is derived under IAU resolutions. In order to obtain clearer physical pictures and improve computational efficiency, an analytic approach is employed. A numerical simulation of a Mars mission is conducted and shows that this approach is satisfactory, in particular being good at dealing with perturbations. This shows that the difference between the proper time on the spacecraft and the TCB reaches the level of sub-seconds, and that the main contributions to this transformation come from the Sun's gravitational field and the velocity of the spacecraft in the BCRS.

In this work, we only examine solutions to the two-body problem, which makes the relative deviations of Mars' gravitational field and the velocity of the spacecraft reach, respectively, about 10^{-7} and 10^{-5}. Our next goal is to include the effect of the three-body disturbing function for the spacecraft.

It is worth noting that there is a long interplanetary journey for a spacecraft before arrival at the target. In this case, the transformation between τ_s and TCB has exactly the same structure as Equation (13), and could be dramatically simplified as

$$\tau_s - t = -\epsilon^2 \int (Gm_\odot/r_{s\odot} + v_s^2/2)\mathrm{d}t$$

when the probe is far beyond the Hill sphere of any massive body except the Sun. Therefore, the final behavior of $\tau_s - t$ during this phase is strongly dependent on the trajectory the spacecraft takes. However, most spacecraft spend their time in quiet mode until crucial orbital maneuvers or scientifically important flybys. For this reason, we do not take much notice of this issue, so it is easy to handle.

References

Anderson, J. D., Campbell, J. K., Ekelund, J. E., Ellis, J., & Jordan, J. F. 2008, Physical Review Letters, 100, 091102

Anderson, J. D., Laing, P. A., Lau, E. L., et al. 1998, Physical Review Letters, 81, 2858

Archinal, B. A., A'Hearn, M. F., Bowell, E., et al. 2011, Celestial Mechanics and Dynamical Astronomy, 109, 101

Bertotti, B., Iess, L., & Tortora, P. 2003, Nature, 425, 374

Blanchet, L., Faye, G., & Ponsot, B. 1998, Phys. Rev. D, 58, 124002

Brumberg, V. A., & Kopejkin, S. M. 1989, Nuovo Cimento B Serie, 103, 63

Chandrasekhar, S. 1965, ApJ, 142, 1488

Damour, T., Soffel, M., & Xu, C. 1991, Phys. Rev. D, 43, 3273

Fehlberg, E. 1968, NASA Technical Report, R-287

IAU Resolutions adopted at the XXVIth General Assembly of the IAU (2006), Resolution 3 Re237 Definition of Barycentric Dynamical Time, TDB

Klioner, S. A., & Soffel, M. H. 2000, Phys. Rev. D, 62, 024019

Kopeikin, S., & Vlasov, I. 2004, Phys. Rep., 400, 209

Murray, C. D., & Dermott, S. F. 2000, Solar System Dynamics (Cambridge Univ. Press)

Petit, G., & Luzum, B. 2010, IERS Conventions 2010, IERS Technical Note 36, Verlag des Bundesamts für Kartographie und Geodäsie (Germany: Frankfurt am Main)

Ping, J., et al. 2009, in APCC 2009, Open Loop Tracking in 1st Chinese Mars Exploration Mission: Yinghuo-1 Martian Orbiter, Communications (15th Asia-Pacific Conference Publications), 446

Soffel, M., Klioner, S. A., Petit, G., et al. 2003, AJ, 126, 2687

Standish, E. M., Newhall, X. X., Williams, J. G., & Yeomans, D. K. 1992, Explanatory Supplement to the Astronomical Almanac, ed. P. K. Seidelmann (Mill Valley: CA), 279

Xie, Y., & Kopeikin, S. 2010, Acta Physica Slovaca, 60, 393